Title

The microRNA cluster miR-17~92 promotes TFH cell differentiation and represses subset-inappropriate gene expression

Journal

Nature Immunology, 14(8)

ISSN

1529-2908

Authors

Baumjohann, Dirk
Kageyama, Robin
Clingan, Jonathan M
et al.

Publication Date

2013-08-01

DOI

10.1038/ni.2642

Peer reviewed

HHS Public Access

Author manuscript

Nat Immunol. Author manuscript; available in PMC 2014 February 01.

Published in final edited form as:

Nat Immunol. 2013 August ; 14(8): 840–848. doi:10.1038/ni.2642.

miR-17~92 promotes T follicular helper cell differentiation and represses subset-inappropriate gene expression

Dirk Baumjohann[1], **Robin Kageyama**[1], **Jonathan M. Clingan**[2,3], **Malika M. Morar**[4], **Sana Patel**[1], **Dimitri de Kouchkovsky**[4], **Oliver Bannard**[5], **Jeffrey A. Bluestone**[4,6], **Mehrdad Matloubian**[2], **K Mark Ansel**[1,7], and **Lukas T. Jeker**[4,6,7]

[1]Department of Microbiology & Immunology, Sandler Asthma Basic Research Center, University of California San Francisco, San Francisco, CA 94143, USA

[2]Division of Rheumatology, Department of Medicine, and Rosalind Russell Medical Research Center for Arthritis, University of California, San Francisco, San Francisco, CA 94143, USA

[3]Graduate Program in Biomedical Sciences, University of California, San Francisco, CA 94143, USA

[4]Diabetes Center and Department of Medicine, University of California San Francisco, San Francisco, CA 94143, USA

[5]Department of Microbiology & Immunology, Howard Hughes Medical Institute, University of California, San Francisco, CA 94143, USA

[6]Department of Pathology, University of California San Francisco, San Francisco, CA 94143, USA

Abstract

T follicular helper (T_{FH}) cells are the prototypic helper T cell subset specialized to enable B cells to form germinal centers and produce high-affinity antibodies. We found that miRNA expression by T cells was essential for T_{FH} cell differentiation. More specifically, we show that after protein immunization the microRNA cluster miR-17~92 was critical for robust T_{FH} cell differentiation and function in a cell-intrinsic manner that occurred regardless of changes in proliferation. In a viral infection model, miR-17~92 restrained the expression of T_{FH} subset-inappropriate genes, including the direct target RAR-related orphan receptor alpha (*Rora*). Genetically removing one *Rora* allele partially rescued the inappropriate gene signature in miR-17~92-deficient T_{FH} cells. Our results identify the miR-17~92 cluster as a critical regulator of T cell-dependent antibody responses, T_{FH} cell differentiation and the fidelity of the T_{FH} cell gene expression program.

Correspondence should be addressed to L.T.J. (ljeker@diabetes.ucsf.edu) or K.M.A. (mark.ansel@ucsf.edu)..

[7]equal contribution

Accession codes Microarray data has been deposited under GEO accession number GSE42760.

Author Contributions D.B. performed and analyzed most of the experiments. R.K., J.M.C., M.M.M., S.P., D.dK., O.B., M.M., and L.T.J. performed and analyzed some of the experiments. J.A.B. interpreted the data. D.B., K.M.A., and L.T.J. designed the experiments, interpreted the data, and wrote the manuscript. All authors discussed the results and commented on the manuscript.

INTRODUCTION

T cell-dependent antibody responses are a pillar of adaptive immunity; they constitute protective responses against a wide variety of pathogens, form the basis of the immune memory induced by the vast majority of effective vaccines, and underlie the pathogenesis of many autoimmune and allergic disorders[1, 2]. T follicular helper (T_{FH}) cells are a subset of $CD4^+$ T cells specialized to provide signals that induce B cell growth, differentiation, immunoglobulin isotype switching, affinity maturation, and antibody secretion[1]. They are defined by Bcl-6, a transcriptional repressor that is necessary and sufficient to direct T_{FH} cell differentiation[3–5], and by abundant expression of the chemokine receptor CXCR5 and PD-1 (ref. [1]). T_{FH} cell differentiation begins very early in the immune response, coinciding with rapid proliferation that expands the pool of responding cells. Bcl-6 is induced very early during T cell activation and is further upregulated in developing T_{FH} cells[6] in conjunction with upregulation of CXCR5 and downregulation of CCR7 (ref. [7]). These changes in homing receptor expression allow developing T_{FH} cells to migrate to the boundary between the T cell zone and B cell follicles of secondary lymphoid organs, where they encounter antigen specific B cells[1]. Continued cognate interactions with antigen-presenting germinal center (GC) B cells within lymphoid follicles further polarize T_{FH} cells[8] and help to maintain the T_{FH} cell phenotype[9]. Besides their established role in orchestrating humoral immunity, T_{FH} cells and transient T_{FH}-like transition states of activated $CD4^+$ T cells have been implicated in the course of T_H1 cell differentiation[10, 11] and the generation of central memory T cells[12, 13].

MicroRNAs have emerged as important regulators of many aspects of immune cell differentiation and function[14]. The cell fate decisions of activated T helper cells are very sensitive to precise dosing of regulatory factors[10], and are therefore subject to regulation by the fine-tuning activity of miRNAs. There is some evidence that miRNAs regulate the T_{FH} cell gene expression program[5] and the plasticity of T_{FH} cells[15]. However, the contribution of miRNAs to T_{FH} cell differentiation and function remains largely unknown.

Here we show that global miRNA expression in $CD4^+$ T cells was absolutely required for the differentiation of T_{FH} cells *in vivo*, independent of any proliferative defects associated with miRNA deficiency. Furthermore, we found that the miR-17~92 cluster was particularly important for robust T_{FH} cell responses. In a protein immunization model, miR-17~92 contributed to the differentiation of an early $CXCR5^{hi}Bcl\text{-}6^{hi}$ T_{FH} cell population, in part by targeting *Pten*. In a viral infection model, miR-17~92 repressed T_{FH} subset-inappropriate gene expression. In this regard, we identified and validated *Rora* as a direct miR-17~92 target that contributed to the pronounced phenotypic changes observed. We conclude that miRNAs are very important regulators of T_{FH} cell differentiation and function.

RESULTS

miRNAs are essential for T_{FH} cell differentiation and function

To investigate the global role of miRNAs in T_{FH} cell differentiation and function we transferred naïve, congenically marked ($CD45.2^+$) miRNA-deficient *Dgcr8*$^{\Delta/\Delta}$ $CD4^+$ T cells bearing an OT-II transgenic T cell receptor (TCR) specific for Ovalbumin (OVA) or control

miRNA-sufficient (*Dgcr8*$^{+/\Delta}$) OT-II cells into CD45.1^{+} wild-type recipients and subsequently immunized the mice with OVA. miRNA-deficient OT-II cells were severely reduced in the draining lymph nodes 4.5 days post immunization compared to control OT-II cells (Fig. 1a). Among the remaining Dgcr8$^{\Delta/\Delta}$ OT-II cells, the frequency of CXCR5^{hi}PD-1^{hi} T_{FH} cells was substantially reduced compared to transferred control cells (Fig. 1a), while endogenous T_{FH} cell frequencies were very similar in both sets of recipients (Supplementary Fig. 1a). The reduced generation of T_{FH} cells resulted in significantly reduced relative and absolute numbers of FAS^{+}Bcl-6^{+} GC B cells (Fig. 1b). Thus, T cell-intrinsic miRNAs are critical for T_{FH} cell responses and GC formation.

To distinguish between impaired proliferation and a potential intrinsic defect in T_{FH} cell differentiation, we tracked T_{FH} cell generation according to the number of cell divisions in the adoptive transfer model[6]. miRNA-deficient T cells proliferated significantly less than control cells (Fig. 1c and Supplementary Fig. 1b). Early Bcl-6 induction was comparable between miRNA-deficient and control cells, as all proliferating cells upregulated Bcl-6 and maintained less expression for several further cell divisions (Fig. 1c and Supplementary Fig. 1b, compare Dgcr8$^{\Delta/\Delta}$ to non-immunized). However, miRNAs were critical for further upregulation of Bcl-6 in developing T_{FH} cells as they proliferated further (Fig. 1c, compare Dgcr8$^{\Delta/\Delta}$ to control). In addition, miRNA-deficient T cells completely failed to upregulate CXCR5, sustained abnormally high CCR7 expression, failed to accumulate in proximity to B cells at the boundary between the T and B cell zones, and did not enter B cell follicles (Fig. 1c and Supplementary Fig. 1b–e). Thus, miRNAs are essential for T_{FH} cell differentiation and function.

miR-17~92 regulates T_{FH} and germinal center responses

Very little is known about the function of specific miRNAs or miRNA loci in T_{FH} cells. A previous report proposed that Bcl-6 inhibits miR-17~92 expression to prevent it from directly repressing CXCR5 (ref. [5]), which would interfere with T cell migration and inhibit T_{FH} cell generation and function. However, T cell activation induces miR-17~92 expression[16, 17] and overexpression of miR-17~92 in lymphocytes leads to a lupus-like autoimmune syndrome with elevated antibody titers, hinting at elevated T_{FH} function[18]. To directly test whether miR-17~92 inhibits or promotes T_{FH} cell generation, we infected mice lacking miR-17~92 only in T cells (CD4-Cre^{+}miR-17~92$^{fl/fl}$; hereafter T17~92$^{\Delta/\Delta}$) with lymphocytic choriomeningitis virus (LCMV). Compared to T17~92$^{+/+}$ control mice, T17~92$^{\Delta/\Delta}$ mice exhibited a pronounced reduction in splenic T_{FH} cells and a severe impairment in GC B cell generation (Fig. 2a), together with an overall reduction in spleen cellularity and the frequency of activated (CD44^{hi}) T cells (Supplementary Fig. 2a,b). Although T17~92$^{\Delta/\Delta}$ mice also lack miR-17~92 in the cytotoxic CD8^{+} T cells that mediate LCMV clearance at this stage of disease, viral clearance was similar at day 8 post infection in T17~92$^{\Delta/\Delta}$ and control mice (data not shown). Thus the impaired antiviral T_{FH} response was not an indirect consequence of reduced viral clearance. Of note, deletion of one copy of the miR-17~92 cluster in T17~92$^{+/\Delta}$ mice resulted in an intermediate phenotype (Fig. 2a and Supplementary Fig. 2a,b).

Using nitrophenyl (NP)-OVA protein immunization as a second, non-infectious model we confirmed that T cell-expressed miR-17~92 was required for T_{FH} cell differentiation and indirectly for GC B cell formation (Fig. 2b). Again, deletion of one copy of the miR-17~92 cluster in T17~92$^{+/\Delta}$ mice resulted in an intermediate phenotype (Fig. 2b). In contrast to the LCMV model, draining lymph node cellularity and total activated T cell numbers were similar in T17~92$^{\Delta/\Delta}$ and control mice (Supplementary Fig. 2c,d), indicating a specific defect in T_{FH} cell generation. This defect resulted in delayed and significantly reduced NP-specific antibody titers (Fig. 2c), and a similar trend was observed in LCMV antibody responses (Supplementary Fig. 2e). In summary, T cell-intrinsic miR-17~92 is required for optimal T_{FH} and germinal center responses including antigen-specific antibody production.

Robust T_{FH} cell differentiation depends on miR-17~92

Although overexpression of miR-17~92 cluster miRNAs promotes T cell proliferation[17–19], adoptively transferred naïve CD4$^+$ T cells displayed only marginally reduced (T17~92$^{\Delta/\Delta}$) or unchanged (T17~92$^{+/\Delta}$) proliferation compared with miR-17~92-sufficient control cells (Fig. 3a, Supplementary Fig. 3a). T17~92$^{\Delta/\Delta}$ cells also proliferated slightly less than control cells when activated with low amounts of anti-CD28 costimulation *in vitro*. However, this defect could be overcome by increasing amounts of anti-CD28 costimulation (Supplementary Fig. 3b). Thus, the miR-17~92 cluster is largely dispensable for T cell proliferation under these conditions, possibly due to partial compensation by the closely related miR-106a~363 and miR-106b~25 clusters.

In contrast, transferred miR-17~92-deficient OT-II cells displayed severely reduced frequencies and total numbers of CXCR5$^+$Bcl-6$^+$ developing T_{FH} cells (Fig. 3b). Tracking the early generation of T_{FH} cells revealed a differentiation defect independent of cell division. Both Bcl-6 and CXCR5 upregulation were impaired in T17~92$^{\Delta/\Delta}$ OT-II cells, resulting in a much smaller proportion of CXCR5$^+$Bcl-6$^+$ developing T_{FH} cells at each cell division compared to miR-17~92-sufficient controls (Fig. 3c,d, Supplementary Fig. 3c). Defective T_{FH} cell differentiation was also reflected by a reduction of IL-21 producing cells (Fig. 3e) and a substantial increase in dividing CXCR5$^-$ cells expressing the high affinity interleukin 2 (IL-2) receptor α chain CD25 (Fig. 3f), which inhibits T_{FH} cell differentiation[20, 21]. T_{FH} cell generation was also reduced among T17~92$^{+/\Delta}$ OT-II cells, indicating that miR-17~92 cluster miRNAs are limiting factors for T_{FH} cell differentiation (Supplementary Fig. 3d). In summary, 17~92$^{\Delta/\Delta}$ CD4$^+$ T cells displayed a T_{FH} cell differentiation defect remarkably similar to that observed in cells lacking all miRNAs, underscoring the prominent functional importance of this particular miRNA cluster.

miR-17~92 overexpression promotes T_{FH} cell generation

Consistent with the idea that T_{FH} differentiation depends on miR-17~92, adoptively transferred OT-II cells overexpressing the cluster in the form of a human transgene (17~92$^{tg/tg}$) showed enhanced T_{FH} cell generation without substantially increased proliferation upon protein immunization (Fig. 4a–d). In unimmunized T17~92$^{tg/+}$ mice, endogenous polyclonal T_{FH} cell numbers were also substantially increased in Peyer's patches, with a corresponding increase in GC B cells (Fig. 4e). Although total B cell and CD4$^+$ T cell numbers were generally increased, GC B cells and T_{FH} cells were preferentially

expanded. Finally, numbers of CXCR5^{hi}PD-1^{hi}Foxp3^{+} T follicular regulatory (T_{FR}) cells (but not polyclonal Treg) correlated with miR-17~92 dosage, suggesting that among all Treg the subset of Treg localized in GCs (T_{FR}) are particularly sensitive to regulation by miR-17~92 (Supplementary Fig. 4). Thus, artificially increasing miR-17~92 enhances T_{FH} cell differentiation and constitutive miR-17~92 overexpression leads to an accumulation of T_{FH} cells.

miR-17~92 represses *Pten* early in T_{FH} cell differentiation

Pten has been implicated as an important contributing target in miR-17~92 overexpressing disease models of autoimmunity and lymphomagenesis[18, 22, 23]. 17~92$^{\Delta/\Delta}$ OT-II cells exhibited significantly elevated PTEN expression in all responding cells at 48 h post-immunization (Supplementary Fig. 5a), and especially in the first few cell divisions at later time points (Supplementary Fig. 5b). Conversely, 17~92$^{tg/tg}$ OT-II cells exhibited reduced PTEN expression (Supplementary Fig. 5c). To test the functional relevance of miR-17~92-mediated repression of PTEN, we genetically limited *Pten* to one allele. Deletion of one allele of *Pten* reduced PTEN expression (Supplementary Fig. 5d) and partially rescued Bcl-6 and CXCR5 induction in early cell divisions of 17~92$^{\Delta/\Delta}$ *Pten*$^{+/\Delta}$ OT-II cells (Supplementary Fig. 5e). However, 17~92$^{\Delta/\Delta}$ *Pten*$^{+/\Delta}$ and 17~92$^{\Delta/\Delta}$ OT-II T cells displayed similar frequencies of CXCR5^{+}Bcl-6^{+} cells at later divisions, suggesting important contributions from additional targets.

miR-17~92 represses T_{FH} cell inappropriate genes

Although the repression of individual miRNA target genes is generally modest, the aggregate biological impact can be large[24, 25]. To obtain a sufficient number of T_{FH} cells for genome-wide transcript analysis, we transferred SMARTA (SM) LCMV-specific TCR-transgenic CD4^{+} T cells into wild-type recipients, infected them with LCMV and then purified T_{FH} cells for microarray analysis (Fig. 5a). The number of 17~92$^{\Delta/\Delta}$ SM T_{FH} cells was also reduced in this system, which was due to a proportional overall reduction in SMARTA cells (Supplementary Fig. 6). Genome-wide transcript analysis showed that as a group, predicted mRNA targets[26] of each miRNA family within the miR-17~92 cluster were derepressed in 17~92$^{\Delta/\Delta}$ SM T_{FH} cells (Fig. 5b). In contrast, predicted miR-29 targets previously shown to be actively repressed by miR-29 in T cells were unaffected in 17~92$^{\Delta/\Delta}$ SM T_{FH} cells[19]. Moderately upregulated mRNAs were enriched for predicted miR-17~92 targets (Supplementary Tables 1,2). In addition, 17~92$^{\Delta/\Delta}$ SM T_{FH} cells showed a striking increase in a recognizable set of T_{FH} cell-inappropriate genes including *Ccr6*, *Il1r2*, *Il1r1*, *Rora*, and *Il22* (Fig. 5c and Supplementary Table 1). Increased protein expression was validated for CCR6 and IL-1R2 by flow cytometry. Both were highly expressed in many 17~92$^{\Delta/\Delta}$ SM T_{FH} cells but only in a few CXCR5^{-} 17~92$^{\Delta/\Delta}$ non- T_{FH} cells (Fig. 5a,d). The majority of these non-T_{FH} cells were T-bet^{hi} $T_{H}1$ cells (data not shown). Additional gene dysregulation in T_{FH} cells was confirmed by qPCR. *Il1r1* and *Rora* were derepressed in 17~92$^{\Delta/\Delta}$ SM T_{FH} cells (Fig. 5e). *Ex vivo* re-stimulation of SMARTA cells also revealed striking increases in the proportion of IL-22^{+}IL-17A^{-} cells and to a lesser extent IL-22^{+}IL-17A^{+} cells, but no increase in IL-17A^{+} single-producing cells (Fig. 5f). Thus, miR-17–92 repressed *Ccr6*, *Il1r2*, *Il1r1*, *Rora* and *Il22* during T_{FH} differentiation. However,

it remained unclear if those genes were directly targeted by miR-17~92 or whether the observed dysregulation was an indirect effect.

Rora is a functionally relevant miR-17~92 target

Rora encodes the RAR-related orphan receptor alpha **(**RORα). Since this nuclear receptor is sufficient to induce IL-1R1 (ref. [27]) and CCR6 (ref. [28]), and IL-1R1 (ref. [27]) partially depends on RORα, we considered the possibility that unrestrained RORα expression may account for part of the observed subset-inappropriate gene expression in 17~92$^{\Delta/\Delta}$ T_{FH} cells. The *Rora* 3′ UTR contains two clusters of predicted miRNA binding sites, each including four conserved miR-17~92 binding sites (Supplementary Fig. 7). Transfection of primary wild-type and 17~92$^{\Delta/\Delta}$ T cells with luciferase reporter constructs showed that endogenous miR-17~92 repressed both clusters, while miR-17~92 overexpressing T cells displayed enhanced repression (Fig. 6a). We isolated the effect of each miRNA by co-transfecting miRNA-deficient T cells with reporter constructs and individual miRNA mimics. This analysis revealed perfect correlation between target site predictions and repressive activity of the corresponding miRNAs (Fig. 6b). We conclude that all 4 miRNA families represented in the miR-17~92 cluster contribute to a robust inhibition of *Rora* expression.

To test the functional relevance of miR-17~92-mediated *Rora* repression *in vivo*, we genetically limited *Rora* to one functional allele by intercrossing SMARTA T17~92$^{\Delta/\Delta}$ and *staggerer* mice that carry a spontaneous mutant allele (*Rora*^{sg}) that does not encode a functional RORα protein. *Rora* heterozygosity in 17~92$^{\Delta/\Delta}$ SM T_{FH} cells restored *Rora* mRNA to the abundance observed in 17~92$^{+/+}$ SM T_{FH} cells (Supplementary Fig. 8). Adoptive transfer of SMARTA 17~92$^{\Delta/\Delta}$ cells with subsequent LCMV infection led to increased CCR6 and IL-1R2 expression predominantly in T_{FH} cells, confirming our previous results (Fig. 6c). In contrast, many fewer 17~92$^{\Delta/\Delta}$ *Rora*$^{+/sg}$ SMARTA cells displayed increased CCR6 expression (Fig. 6c). Thus, limiting *Rora* partially restored proper regulation of CCR6 despite the absence of miR-17~92. Importantly, neither wild-type, 17~92$^{\Delta/\Delta}$, nor 17~92$^{\Delta/\Delta}$ *Rora*$^{+/sg}$ T_{FH} cells showed differences in the expression of the closely related ROR family member RORγt, which can also induce CCR6 expression (Fig. 6d). Microarray experiments also indicated no significant difference in the expression of RORγt in control and 17~92$^{\Delta/\Delta}$ SMARTA T_{FH} cells (data not shown). Thus, it is unlikely that RORγt was the driving force behind the dysregulated gene signature of 17~92$^{\Delta/\Delta}$ T_{FH} cells. IL-1R2 expression was not affected by limiting *Rora* (Fig. 6c). However, the frequency of IL-22 producing SMARTA 17~92$^{\Delta/\Delta}$ *Rora*$^{+/sg}$ cells was also reduced by about half compared to SMARTA 17~92$^{\Delta/\Delta}$ cells (Fig. 6e). We conclude that miR-17~92 is required to directly repress *Rora* during T_{FH} differentiation in order to prevent subset-inappropriate gene expression.

DISCUSSION

A better understanding of the genetic programs that regulate T_{FH} cell differentiation and plasticity might lead to novel strategies for rational vaccine design and suppression of antibody-mediated autoimmune diseases. Major advances deciphering important roles for Bcl-6 and other protein-coding genes have been achieved in recent years[1]. In contrast, very

little is known about the role of miRNAs in T_{FH} cell differentiation. We found that miRNAs are absolutely critical for T_{FH} cell differentiation and function, and that the miR-17~92 cluster in particular is required for robust T_{FH} responses in a T cell-intrinsic manner. Those SM T_{FH} cells that did develop in the absence of miR-17~92 failed to suppress the direct target *Rora* and a suite of other T_{FH} cell-inappropriate genes normally expressed in T_H17 and T_H22 cells. We conclude that miR-17~92 promotes T_{FH} cell differentiation and maintains the fidelity of T_{FH} cell identity by repressing non-T_{FH} cell genes both directly and indirectly. Taken together with previous studies that demonstrated miR-17~92 regulation of T cell proliferation and survival[17–19], our findings indicate that miR-17~92 constitutes a central coordinator of activated T cell fate decisions.

The global role of miRNAs in T_{FH} cell responses has been difficult to study because of the strong defects in T cell survival and proliferation in miRNA-deficient T cells. We overcame this roadblock using adoptive transfer of OVA-specific OT-II TCR transgenic T cells and intravital dye dilution to analyze the early stages of T_{FH} differentiation in miRNA-sufficient and miRNA-deficient cells that had survived and divided the same number of times *in vivo*. This approach revealed that miRNAs are essential for the earliest steps in T_{FH} cell differentiation, including upregulation of Bcl-6 and CXCR5, downregulation of CCR7, and migration to sites of interaction with B cells in secondary lymphoid organs. These findings contrast sharply with the requirement for miRNAs to restrain T_H1 differentiation[19, 29], but are reminiscent of the requirement for miRNAs in supporting Treg differentiation and function[30–32].

The same transfer system revealed that miR-17~92 regulates multiple T cell behaviors that are important for mounting effective humoral immune responses. miR-17~92 had a surprisingly small effect on the proliferation of OT-II T cells *in vivo*, but it was clearly required for optimal T_{FH} cell differentiation. Increased expression of *Pten*, a known direct target of miR-17~92 and regulator of T_{FH} cell responses[18, 33], partially accounted for defective T_{FH} cell generation during the earliest cell divisions. Interestingly, CD28 costimulation represses PTEN[34] and induces miR-17~92 expression in activated T cells[16] (D.d.K., J.A.B. and L.T.J., unpublished observations). We speculate that the required role of CD28 costimulation in T_{FH} cell differentiation[35] may be mediated in part by miR-17~92 induction and subsequent PTEN downregulation. However, the effect of *Pten* regulation was barely detectable in this system, indicating important roles for other direct targets of miR-17~92. Cell proliferation and the early wave of Bcl-6 induction that occurs in all activated T cells[6] was intact in the absence of miR-17~92. These observations indicated that some of the relevant targets must affect T_{FH} cell differentiation per se rather than T cell activation in general. In contrast, the more prominent second phase of Bcl-6 upregulation characteristic of T_{FH} cells was severely blunted, and CXCR5 induction was almost completely abrogated. We also observed specific effects on T_{FH} cell differentiation that could be clearly distinguished from general activation defects in LCMV infection. $17\sim92^{\Delta/\Delta}$ SM T_{FH} cells acquired an inappropriate gene expression program reminiscent of T_H17 or T_H22 cells[4, 36], including upregulation of RORα, CCR6, components of the IL-1 pathway (IL-1R1, IL-1R2), and inducible production of IL-22. T_H17 and T_H22 cells are closely related T_H subsets that display many shared (for example, CCR6 expression) but also

distinct features[37, 38]. However, T17~92$^{\Delta/\Delta}$ T_{FH} cells did not convert into RORγt^{+} and IL-17-producing T_H17 cells, nor did they become proper T_H22 cells. Instead, they maintained expression of the T_{FH} cell program, including the markers CXCR5, Bcl-6, and PD-1, and became a hybrid cell type with molecular features of more than one helper T cell subset. We conclude that T_{FH} cells require miR-17~92 to repress inappropriate non-T_{FH} gene expression programs. This requirement was selective for T_{FH} cells, since CCR6 and IL-1R2 expression were much less affected in non-T_{FH} cells (which are mostly T_H1 cells) in the same infected spleens.

We noted that miR-17~92 deficiency did not affect the frequency of SMARTA T_{FH} cells, but did significantly reduce the total number of both T_{FH} cells and T_H1 cells in infected spleens. Thus LCMV, which induces extremely robust T cell expansion, revealed the defect in *in vivo* antigen-driven helper T cell proliferation that was predicted by previous *in vitro* studies[18, 19], whereas the slower proliferating OT-II transgenic T cells manifested a more selective defect in T_{FH} cell differentiation. Polyclonal responses in T17~92$^{\Delta/\Delta}$ mice also differed in the magnitude of the defect in the frequency and number of T_{FH} cells (more affected in LCMV infection) and GC B cells (more affected in OVA immunization). Compromised function of CD8^{+} T cells, which also lack miR-17~92 in these mice, may indirectly affect these responses, particularly in the case of LCMV infection[39].

CD4^{+} T helper cell “plasticity” has garnered a lot of attention in recent years. Current models of T cell differentiation suggest that cell identity is less rigid than previously thought[40]. Although Bcl-6 has been identified as a subset-defining transcription factor required for T_{FH} cell differentiation[3–5], it remains controversial whether or not T_{FH} cells represent a stable cell lineage[1]. A recent model suggests that initial helper T cell differentiation proceeds via a Bcl-6^{+} pre-T helper cell stage with concomitant expression of T-bet, GATA3 and/or RORγt[41]. According to this model, T_H1, T_H2, or T_H17 differentiation cues downregulate Bcl-6 and further upregulate the lineage-defining factors, increased Bcl-6 expression and suppression of RORγt, GATA3 and T-bet yields T_{FH} cells. Since concomitant expression of competing transcription programs are common, repression of genes leading to alternative cell fates is an important requirement during T cell differentiation[10, 42]. Individual miRNAs can be powerful enough to shift a cell’s transcriptome to that of a different cell type[43], and they maintain the fidelity of cell-type specific transcriptomes by repressing genetic programs of other cell lineages[44]. We previously reported that miRNA deficiency induces proinflammatory cytokine secretion in Treg even though they continue to express Foxp3 (ref. [30]). miR-10a may restrict the plasticity of several subsets of helper T cells, including both Treg and T_{FH} cells, and may influence T_H17 differentiation[15, 45]. miR-29 prevents aberrant activation of the T_H1 program by repressing both T-bet and its homolog Eomesodermin, which is usually not expressed in CD4^{+} T cells[19]. In this study, we found that all four miRNA families in the miR-17~92 cluster target *Rora* to prevent the expression of CCR6 and other genes associated with T_H17 or T_H22 cells. Thus, a paradigm is emerging in which miRNAs help to define and maintain cell identity by repressing alternative gene expression programs, effectively limiting the plasticity of differentiating T cells.

Interestingly, while a dichotomy between T_{FH} and T_H17 differentiation pathways has been proposed[4], T_H17 cells can acquire a T_{FH} phenotype under certain conditions in Peyer's patches[46]. The unexpected identification of RORα as a direct miR-17~92 target and functionally relevant contributor to T_{FH}-inappropriate gene expression suggests that differentiating (pre-)T_{FH} cells receive signals that induce *Rora* transcription, but that miR-17~92 renders that induction inconsequential. Future studies will be needed to identify those signals and to test whether miR-17~92 controls RORα expression in other cell types as well. A "lineage-defining" transcription factor has not been identified for T_H22 cells but we note that despite their similarity to T_H17 cells expression of RORγt is not required for human T_H22 cells[36]. In line with this, RORγt expression was not significantly affected in the hybrid $T_{FH}/T_H17/T_H22$ signature we found in $17\sim92^{\Delta/\Delta}$ SM T_{FH} cells. Moreover, T_H17 cell heterogeneity poses specific challenges and certain types of T_H17 cells might be more closely related to T_H22 cells than conventional T_H17 cells[38]. Thus, the distinct functions of RORα and RORγt in differentiating T cells might need to be revisited. In addition, it remains uncertain whether altered migration, response to cytokines, or some other trait of RORα expressing cells limits T_{FH} differentiation and function *in vivo*. Future studies are required to define miR-17~92 function in early T_{FH} cell fate determination and to dissect cell intrinsic effects on the molecular program from secondary effects due to altered abilities to sense the environment. Finally, it is important to note that our data demonstrate that regulation of RORα only partially explains the hybrid gene expression profile in miR-17~92-deficient T_{FH} cells. Additional direct targets relevant to this phenotype must exist and remain to be discovered. Nevertheless, our findings indicate that miR-17~92 and Bcl-6 cooperate to imprint and protect the identity of developing T_{FH} cells by repressing differentiation into alternate T cell subsets.

METHODS

Mice

TCR-transgenic (tg) OT-II (004194), floxed miR-17~92 (008458), Rosa26-miR-17~92 tg (008517), and heterozygous *Rora*^{sg} (002651) mice were purchased from The Jackson Laboratory (JAX). CD4-Cre mice (4196) were obtained from Taconic. OT-II and SMARTA [47] mice were crossed with B6.SJL-Ptprca Pepcb/BoyJ mice (002014) to obtain offspring with congenic CD45 alleles. Floxed *Dgcr8* (ref. [48]) mice were kindly provided by R. Blelloch. C57BL/6 (JAX) or congenic B6-LY5.2/Cr (National Cancer Institute) mice were used as recipients. Floxed *Pten* mice have been described before[49]. All experiments were done according to the Institutional Animal Care and Use Committee guidelines of the University of California, San Francisco.

Adoptive cell transfers, infections, and immunizations

OT-II and SMARTA cells were pre-enriched from spleens and lymph nodes (LNs) with the $CD4^+$ negative isolation kit (Invitrogen) and naïve T cells ($CD4^+CD8^-CD25^-CD44^{low}CD62L^{hi}$) were further purified on a FACS Aria II cell sorter (BD Biosciences). To obtain true *Dgcr8*-deficient OT-II cells, naïve cells were additionally sorted according to YFP expression driven by a Rosa26-YFP reporter allele, in which efficient excision of a floxed stop cassette by the CD4-Cre activity results in a bright YFP

signal. For cell proliferation experiments, naïve T cells were labeled with 5 μM CellTrace Violet (Invitrogen) as described before[6]. NP_{18}-OVA (Biosearch Technologies) was mixed with Imject Alum (Pierce) and 5 μg NP_{18}-OVA were injected s.c. into each hind footpad or 50 μg s.c. in the base of tail and flank. In some experiments, mice were infected i.p. with 2×10^5 PFU lymphocytic choriomeningitis virus (Armstrong strain).

Flow cytometry

Spleen and LN cells were gently disrupted between the frosted ends of microscope slides and single-cell suspensions were filtered through fine mesh. Antibodies were purchased from eBioscience, BD Biosciences, or Biolegend: CD4 (clone RM4–5), CD8α (53-6.7), CD19 (1D3), CD25 (PC61.5), CD45.1 (A20), CD45.2 (104), CD44 (IM7), CD62L (MEL-14), CCR6 (140706), B220 (RA3–6B2), FAS (Jo2), GL-7, IgD (11–26c), IL-17A (eBio17B7), IL1R2 (4E2), IL-22 (1H8PWSR), PD-1 (J43 or RMP1–30). Unspecific binding was blocked with anti-CD16/CD32 plus 2% normal mouse/rat serum. Biotinylated anti-CXCR5 (clone 2G8, BD Biosciences) was visualized with streptavidin-allophycocyanin. Staining with biotinylated anti-CCR7 (clone 4B12, eBioscience) was performed for 30 min at 37 °C, followed by regular surface staining including streptavidin-allophycocyanin at 4 °C. The anti-Bcl-6 mAb (clone K112-91), anti-PTEN mAb (clone A2B1), and anti-RORγt mAb (clone Q31–378) were from BD Biosciences. Intracellular Bcl-6 staining was performed with the Foxp3 Staining Set (eBioscience). Cytofix Fixation Buffer and Perm Buffer III (BD) were used for intracellular PTEN staining. For intracellular cytokine staining, LN cells were stimulated with PMA/ionomycin for 4h, with the addition of Brefeldin A for the last 2h. Cells were fixed with 4% paraformaldehyde followed by permeabilization with saponin (Sigma-Aldrich). Human IL-21R–Fc chimera (R&D Systems) was revealed with Phycoerythrin-labeled Fc-specific anti-human IgG F(ab')2 fragments (Jackson ImmunoResearch). Samples were acquired on a LSR II cytometer (BD Biosciences) and analyzed with FlowJo software (Tree Star), gating out doublets as well as non-T or non-B cells, where appropriate, in a dump channel. Dead cells were excluded with 7-aminoactinomycin D (eBioscience) or Fixable Viability Dye eFluor780 (eBioscience).

In vitro co-stimulation and proliferation assay

Naïve T cells from control and CD4-Cre^+miR17~$92^{fl/fl}$ mice were activated *in vitro* with plate-bound anti-CD3 (clone 2C11)/anti-CD28 (PV1) for 48 h and 72 h. CFSE-labeling was performed as described[50]. Proliferation analysis was performed using the proliferation analysis function in FlowJo for Mac V9.2 and higher. To normalize for interexperimental differences we normalized all data to the control in the first experiment (defined as a proliferative index of 1).

RNA extraction and quantitative real-time PCR

RNA extraction and miRNA qPCR was performed as described before[45].

Microarrays

Naïve SMARTA cells were purified by flow cytometry from T17~$92^{+/+}$ control or T17~$92^{\Delta/\Delta}$ donor mice and adoptively transferred into wild-type mice. Recipients were

infected i.p. with LCMV Armstrong and spleens were dissected 5.5 days later. Spleen cells were pooled for each condition (n = 3–5 mice) and $CD4^+$ T cells were enriched with the $CD4^+$ negative isolation kit (Invitrogen) and congenically marked SMARTA T_{FH} cells ($7AAD^-CD4^+CD8^-CD19^-CXCR5^{hi}PD\text{-}1^{hi}$) were sorted directly into Trizol LS reagent and stored at −80°C until further processing. RNA from four independent experiments was purified using RNeasy columns (Qiagen). Sample preparation, labeling, and array hybridizations were performed according to standard protocols from the UCSF Shared Microarray Core Facilities and Agilent Technologies (http://www.arrays.ucsf.edu and http://www.agilent.com). Total RNA quality was assessed using a Pico Chip on an Agilent 2100 Bioanalyzer (Agilent Technologies). RNA was amplified using the Sigma whole transcriptome amplification kits following the manufacturer's protocol (Sigma-Aldrich), and subsequent Cy3-CTP labeling was performed using NimbleGen one-color labeling kits (Roche-NimbleGen Inc,). Labeled Cy3-cDNA was assessed using the Nanodrop ND-8000 (Nanodrop Technologies, Inc.), and equal amounts of Cy3 labeled target were hybridized to Agilent whole mouse genome 8×60K in-jet arrays. Hybridizations were performed for 17h, according to the manufacturer's protocol. Arrays were scanned using the Agilent microarray scanner and raw signal intensities were extracted with Feature Extraction v10.6 software.

Rora 3′′ UTR cloning, T cell transfections and luciferase assays

Two different 3' UTR constructs of *Rora* were cloned into the psiCHECK-2 luciferase reporter construct (Promega) as described in Supplementary Fig. 7. Primer sequences were: P1 F: 5′-TAGTAGCTCGAGATGTCGCGCCCGAGCACTTC-3′; P1 R: 5′-TAGTAGGCGGCCGCAAACAGCAGCATAAATACCTCCCAACG-3′; P2 F: 5′-TAGTAGCTCGAGCCCCCAAAGTCTTTAACATCCTGA-3′; P2 R: 5′-TAGTAGGCGGCCGCAGTCAACCATAAGGTGCTTATTACTATTA-3′.) T cell transfections and luciferase assays were performed as described before[13]. $CD4^+$ T cells from spleen and lymph nodes were isolated by magnetic bead selection (Dynal) and stimulated with anti-CD3 and anti-CD28. Cells were transfected with the Neon electroporation transfection system (Invitrogen). miRIDIAN miRNA mimics (miR-17, miR-18a, miR-19a, miR-92a) and controls were from Dharmacon. Activated $CD4^+$ T cells were transfected with reporter constructs and luciferase activity was measured 24 h after transfection with the Dual Luciferase Reporter Assay System (Promega) and a FLUOstar Optima plate-reader (BMG Labtech).

ELISA

96-well half-area plates (Costar) were coated overnight with 10 μg/ml NP_{24}-BSA (Biosearch Technologies) in PBS at 4 °C. Plates were blocked with 1% BSA in PBS and serial dilutions of serum were incubated at 21°C Horseradish peroxidase (HRP)-conjugated anti-mouse IgG1-specific antibodies (Southern Biotech) and Super AquaBlue ELISA Substrate (eBioscience) were used as detection reagents. Absorbance was measured at 410 nm with a FLUOstar Optima plate-reader (BMG Labtech). Absolute values were calculated according to reference sera derived from hyper-immunized mice and are expressed in arbitrary units (AU). For LCMV-specific antibody measurements, plates were coated with LCMV-infected BHK lysate. After blocking with 10% FBS in PBS, serially diluted serum was added. Anti-mouse IgG-HRP was used as detection antibody (Southern Biotech) with 3,3′,5,5′-

tetramethylbenzidine as substrate. Ab titers were determined as the reciprocal of the dilution that gave an OD value (450 nm) reading of more than 2-fold above that of naive control sera.

Immunohistochemistry

Draining popliteal LNs were dissected, embedded in Tissue-Tek O.C.T compound (Sakura Finetek), and flash-frozen in liquid nitrogen. Frozen tissues were stored at −80 °C until further processing. Cryosections (7 μm) were air-dried for 1h before and after fixation in cold acetone for 10 min, and then were rehydrated in 0.1% BSA containing Tris-buffered saline (TBS pH 7.6) for 10 min. Slides were stained for 3 h at 20–25 °C in a humidified chamber in TBS containing 0.1% BSA, 1% normal mouse serum and 1% normal rat serum with a mixture of the following diluted primary antibodies: CD45.2 FITC (Biolegend), goat anti-mouse IgD (Cedarlane labs). After washing for 5 min in TBS, slides were incubated for 1h with cocktails of the following secondary reagents (all from Jackson Immunoresearch) in TBS/0.1% BSA: mouse anti-FITC alkaline phosphatase (AP), donkey anti-goat horse radish peroxidase (HRP), streptavidin HRP. Enzyme conjugates were developed with DAB and Fast-blue (both from Sigma-Aldrich).

Statistics

Data were analyzed with Prism 5 (GraphPad Software). The two-tailed non-parametric Mann-Whitney test was used to compare two unpaired groups. The non-parametric Kruskal-Wallis test was used to compare three or more unpaired groups, followed by Dunn's post test to calculate *P* values for each group. Two-way ANOVA was used together with Bonferroni post tests to compare replicates in each cell division of CTV-labeled OT-II cells. Graphs show the mean ± SEM. *, $P < 0.05$; **, $P < 0.01$; ***, $P < 0.001$.

Supplementary Material

Refer to Web version on PubMed Central for supplementary material.

Acknowledgements

We thank M. Panduro for technical assistance, R. Blelloch for providing *Dgcr8*$^{fl/fl}$ mice, R. Barbeau, J. Pollack, A. Barczak and D. Erle (SABRE Functional Genomics Core) for expert assistance with microarray experiments, the UCSF miRNA in lymphocyte group for scientific discussions, D. Fuentes for animal husbandry, and D. Le for help with genotyping. This work was supported by the Burroughs Wellcome Fund (CABS 1006173 to K.M.A), NIH grants R01 HL109102, P01 HL107202 (to K.M.A), P01 AI35297, U19 AI056388 (to J.A.B.), P30 DK63720 (for core support), and a Scholar Award from the Juvenile Diabetes Research Foundation (to J.A.B.). D.B. was supported by the Swiss National Science Foundation (PBBEP3-133516) and the Swiss Foundation for Grants in Biology and Medicine (PASMP3-142725). J.M.C. was supported by a Graduate Research fellowship from the National Science Foundation. O.B. was supported by a Sir Henry Wellcome Postdoctoral Fellowship from the Wellcome Trust. L.T.J was supported by the Swiss Foundation for Grants in Biology and Medicine (PASMP3-124274/1).

REFERENCES

1. Crotty S. Follicular helper CD4 T cells (TFH). Annu. Rev. Immunol. 2011; 29:621–663. [PubMed: 21314428]
2. Vinuesa CG, Sanz I, Cook MC. Dysregulation of germinal centres in autoimmune disease. Nat. Rev. Immunol. 2009; 9:845–857. [PubMed: 19935804]

3. Johnston RJ, et al. Bcl6 and Blimp-1 are reciprocal and antagonistic regulators of T follicular helper cell differentiation. Science. 2009; 325:1006–1010. [PubMed: 19608860]
4. Nurieva RI, et al. Bcl6 mediates the development of T follicular helper cells. Science. 2009; 325:1001–1005. [PubMed: 19628815]
5. Yu D, et al. The transcriptional repressor Bcl-6 directs T follicular helper cell lineage commitment. Immunity. 2009; 31:457–468. [PubMed: 19631565]
6. Baumjohann D, Okada T, Ansel KM. Cutting Edge: Distinct waves of BCL6 expression during T follicular helper cell development. J. Immunol. 2011; 187:2089–2092. [PubMed: 21804014]
7. Ansel KM, McHeyzer-Williams LJ, Ngo VN, McHeyzer-Williams MG, Cyster JG. In vivo-activated CD4 T cells upregulate CXC chemokine receptor 5 and reprogram their response to lymphoid chemokines. J. Exp. Med. 1999; 190:1123–1134. [PubMed: 10523610]
8. Yusuf I, et al. Germinal center T follicular helper cell IL-4 production is dependent on signaling lymphocytic activation molecule receptor (CD150). J. Immunol. 2010; 185:190–202. [PubMed: 20525889]
9. Baumjohann D, et al. Persistent antigen and germinal center B cells sustain T follicular helper cell responses and phenotype. Immunity. 2013; 38:596–605. [PubMed: 23499493]
10. Oestreich KJ, Weinmann AS. Master regulators or lineage-specifying? Changing views on CD4(+) T cell transcription factors. Nat. Rev. Immunol. 2012; 12:799–804. [PubMed: 23059426]
11. Nakayamada S, et al. Early Th1 cell differentiation is marked by a Tfh cell-like transition. Immunity. 2011; 35:919–931. [PubMed: 22195747]
12. Pepper M, Pagan AJ, Igyarto BZ, Taylor JJ, Jenkins MK. Opposing signals from the Bcl6 transcription factor and the interleukin-2 receptor generate T helper 1 central and effector memory cells. Immunity. 2011; 35:583–595. [PubMed: 22018468]
13. Weber JP, Fuhrmann F, Hutloff A. T-follicular helper cells survive as long-term memory cells. Eur. J. Immunol. 2012; 42:1981–1988. [PubMed: 22730020]
14. Xiao C, Rajewsky K. MicroRNA control in the immune system: basic principles. Cell. 2009; 136:26–36. [PubMed: 19135886]
15. Takahashi H, et al. TGF-beta and retinoic acid induce the microRNA miR-10a, which targets Bcl-6 and constrains the plasticity of helper T cells. Nat. Immunol. 2012; 13:587–595. [PubMed: 22544395]
16. Bronevetsky Y, et al. T cell activation induces proteasomal degradation of Argonaute and rapid remodeling of the microRNA repertoire. J. Exp. Med. 2013; 210:417–432. [PubMed: 23382546]
17. Jiang S, et al. Molecular dissection of the miR-17–92 cluster's critical dual roles in promoting Th1 responses and preventing inducible Treg differentiation. Blood. 2011; 118:5487–5497. [PubMed: 21972292]
18. Xiao C, et al. Lymphoproliferative disease and autoimmunity in mice with increased miR-17–92 expression in lymphocytes. Nat. Immunol. 2008; 9:405–414. [PubMed: 18327259]
19. Steiner DF, et al. MicroRNA-29 regulates T-box transcription factors and interferon-gamma production in helper T cells. Immunity. 2011; 35:169–181. [PubMed: 21820330]
20. Ballesteros-Tato A, et al. Interleukin-2 inhibits germinal center formation by limiting T follicular helper cell differentiation. Immunity. 2012; 36:847–856. [PubMed: 22464171]
21. Johnston RJ, Choi YS, Diamond JA, Yang JA, Crotty S. STAT5 is a potent negative regulator of TFH cell differentiation. J. Exp. Med. 2012; 209:243–250. [PubMed: 22271576]
22. Ventura A, et al. Targeted deletion reveals essential and overlapping functions of the miR-17 through 92 family of miRNA clusters. Cell. 2008; 132:875–886. [PubMed: 18329372]
23. Olive V, et al. miR-19 is a key oncogenic component of mir-17–92. Genes & Dev. 2009; 23:2839–2849. [PubMed: 20008935]
24. Ebert MS, Sharp PA. Roles for microRNAs in conferring robustness to biological processes. Cell. 2012; 149:515–524. [PubMed: 22541426]
25. Mendell JT, Olson EN. MicroRNAs in stress signaling and human disease. Cell. 2012; 148:1172–1187. [PubMed: 22424228]
26. Friedman RC, Farh KK, Burge CB, Bartel DP. Most mammalian mRNAs are conserved targets of microRNAs. Genome Res. 2009; 19:92–105. [PubMed: 18955434]

27. Chung Y, et al. Critical regulation of early Th17 cell differentiation by interleukin-1 signaling. Immunity. 2009; 30:576–587. [PubMed: 19362022]
28. Yamazaki T, et al. CCR6 regulates the migration of inflammatory and regulatory T cells. J. Immunol. 2008; 181:8391–8401. [PubMed: 19050256]
29. Muljo SA, et al. Aberrant T cell differentiation in the absence of Dicer. J. Exp. Med. 2005; 202:261–269. [PubMed: 16009718]
30. Zhou X, et al. Selective miRNA disruption in T reg cells leads to uncontrolled autoimmunity. J. Exp. Med. 2008; 205:1983–1991. [PubMed: 18725525]
31. Liston A, Lu LF, O'Carroll D, Tarakhovsky A, Rudensky AY. Dicer-dependent microRNA pathway safeguards regulatory T cell function. J. Exp. Med. 2008; 205:1993–2004. [PubMed: 18725526]
32. Chong MM, Rasmussen JP, Rudensky AY, Littman DR. The RNAseIII enzyme Drosha is critical in T cells for preventing lethal inflammatory disease. J. Exp. Med. 2008; 205:2005–2017. [PubMed: 18725527]
33. Rolf J, et al. Phosphoinositide 3-kinase activity in T cells regulates the magnitude of the germinal center reaction. J. Immunol. 2010; 185:4042–4052. [PubMed: 20826752]
34. Buckler JL, Walsh PT, Porrett PM, Choi Y, Turka LA. Cutting edge: T cell requirement for CD28 costimulation is due to negative regulation of TCR signals by PTEN. J. Immunol. 2006; 177:4262–4266. [PubMed: 16982858]
35. Linterman MA, Vinuesa CG. Signals that influence T follicular helper cell differentiation and function. Semin. Immunopathol. 2010; 32:183–196. [PubMed: 20107805]
36. Duhen T, Geiger R, Jarrossay D, Lanzavecchia A, Sallusto F. Production of interleukin 22 but not interleukin 17 by a subset of human skin-homing memory T cells. Nat. Immunol. 2009; 10:857–863. [PubMed: 19578369]
37. Rutz S, Eidenschenk C, Ouyang W. IL-22, not simply a Th17 cytokine. Immunol. Rev. 2013; 252:116–132. [PubMed: 23405899]
38. Basu R, Hatton RD, Weaver CT. The Th17 family: flexibility follows function. Immunol. Rev. 2013; 252:89–103. [PubMed: 23405897]
39. Wu T, et al. Temporal expression of microRNA cluster miR-17–92 regulates effector and memory CD8+ T-cell differentiation. Proc. Natl. Acad. Sci. USA. 2012; 109:9965–9970. [PubMed: 22665768]
40. O'Shea JJ, Paul WE. Mechanisms Underlying Lineage Commitment and Plasticity of Helper CD4+ T Cells. Science. 327:1098–1102. [PubMed: 20185720]
41. Ma CS, Deenick EK, Batten M, Tangye SG. The origins, function, and regulation of T follicular helper cells. J. Exp. Med. 2012; 209:1241–1253. [PubMed: 22753927]
42. Zhu J, Yamane H, Paul WE. Differentiation of effector CD4 T cell populations. Annu. Rev. Immunol. 2010; 28:445–489. [PubMed: 20192806]
43. Lim LP, et al. Microarray analysis shows that some microRNAs downregulate large numbers of target mRNAs. Nature. 2005; 433:769–773. [PubMed: 15685193]
44. Stark A, Brennecke J, Bushati N, Russell RB, Cohen SM. Animal MicroRNAs confer robustness to gene expression and have a significant impact on 3'UTR evolution. Cell. 2005; 123:1133–1146. [PubMed: 16337999]
45. Jeker LT, et al. MicroRNA 10a Marks Regulatory T Cells. PLoS ONE. 2012; 7:e36684. [PubMed: 22629323]
46. Hirota K, et al. Plasticity of TH17 cells in Peyer's patches is responsible for the induction of T cell-dependent IgA responses. Nat. Immunol. 2013; 14:372–379. [PubMed: 23475182]
47. Oxenius A, Bachmann MF, Zinkernagel RM, Hengartner H. Virus-specific MHC-class II-restricted TCR-transgenic mice: effects on humoral and cellular immune responses after viral infection. Eur. J. Immunol. 1998; 28:390–400. [PubMed: 9485218]
48. Rao PK, et al. Loss of cardiac microRNA-mediated regulation leads to dilated cardiomyopathy and heart failure. Circ. Res. 2009; 105:585–594. [PubMed: 19679836]
49. Suzuki A, et al. T cell-specific loss of Pten leads to defects in central and peripheral tolerance. Immunity. 2001; 14:523–534. [PubMed: 11371355]

50. Tang Q, et al. In vitro-expanded antigen-specific regulatory T cells suppress autoimmune diabetes. J. Exp. Med. 2004; 199:1455–1465. [PubMed: 15184499]

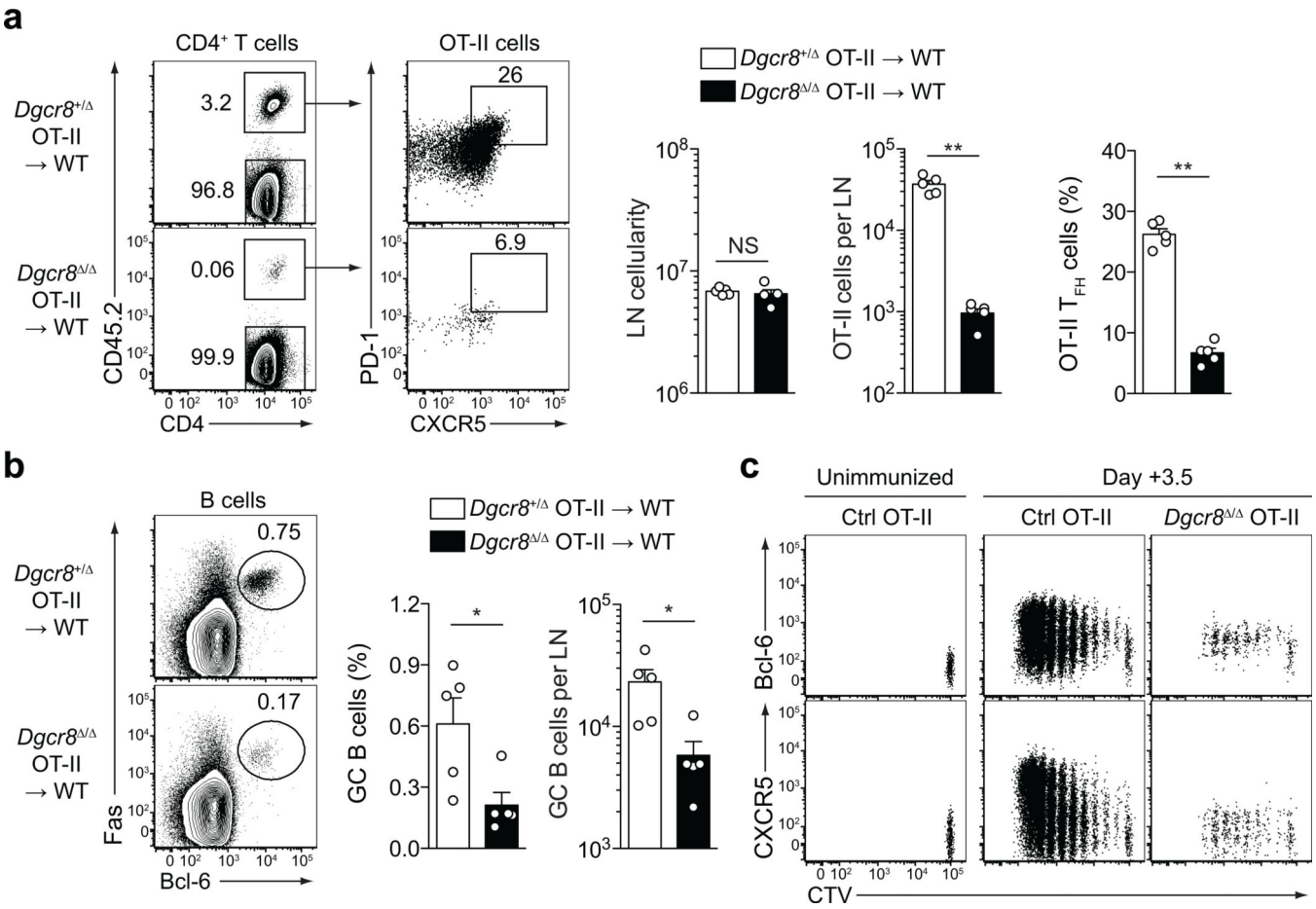

Figure 1. T cell-expressed miRNAs are essential for T_{FH} cell differentiation and germinal center B cell induction

(**a**) Naïve CD45.2$^+$R26-YFP$^+$ OT-II cells from CD4-Cre$^+$Dgcr8$^{+/fl}$ (Dgcr8$^{+/\Delta}$) control or CD4-Cre$^+$Dgcr8$^{fl/fl}$ (Dgcr8$^{\Delta/\Delta}$) donor mice were adoptively transferred into wild-type mice (CD45.1$^+$) and hosts were immunized with NP-OVA/alum subcutaneously (s.c.) in the hind footpads. Draining LNs were analyzed by flow cytometry on day +4.5. Representative contour plots show the frequency of CD45.2$^+$ OT-II cells among total CD4$^+$ T cells as well as the frequency of CXCR5$^+$PD-1$^+$ T_{FH} cells among transferred OT-II cells. Gated on live CD4$^+$B220$^-$ lymphocytes. Data are quantified in the bar graphs with each dot representing one mouse (n = 5). (**b**) Representative contour plots and quantification of GC B cells in the draining LN. B cells were gated as live CD19$^+$B220$^+$ lymphocytes. (**c**) Naïve CD45.2$^+$R26-YFP$^+$ OT-II cells from control or Dgcr8$^{\Delta/\Delta}$ donor mice were labeled with CTV and adoptively transferred into wild-type recipients, followed by OVA/alum immunization in the hind footpads. Draining popliteal LNs were dissected on day +3.5 after immunization and analyzed by flow cytometry for Bcl-6 and CXCR5 expression kinetics. Unimmunized OT-II cell-recipients served as controls. OT-II cells were gated as live CD45.2$^+$CD4$^+$B220$^-$ lymphocytes. Data are representative of three (**a, b**) and five (**c**) independent experiments.

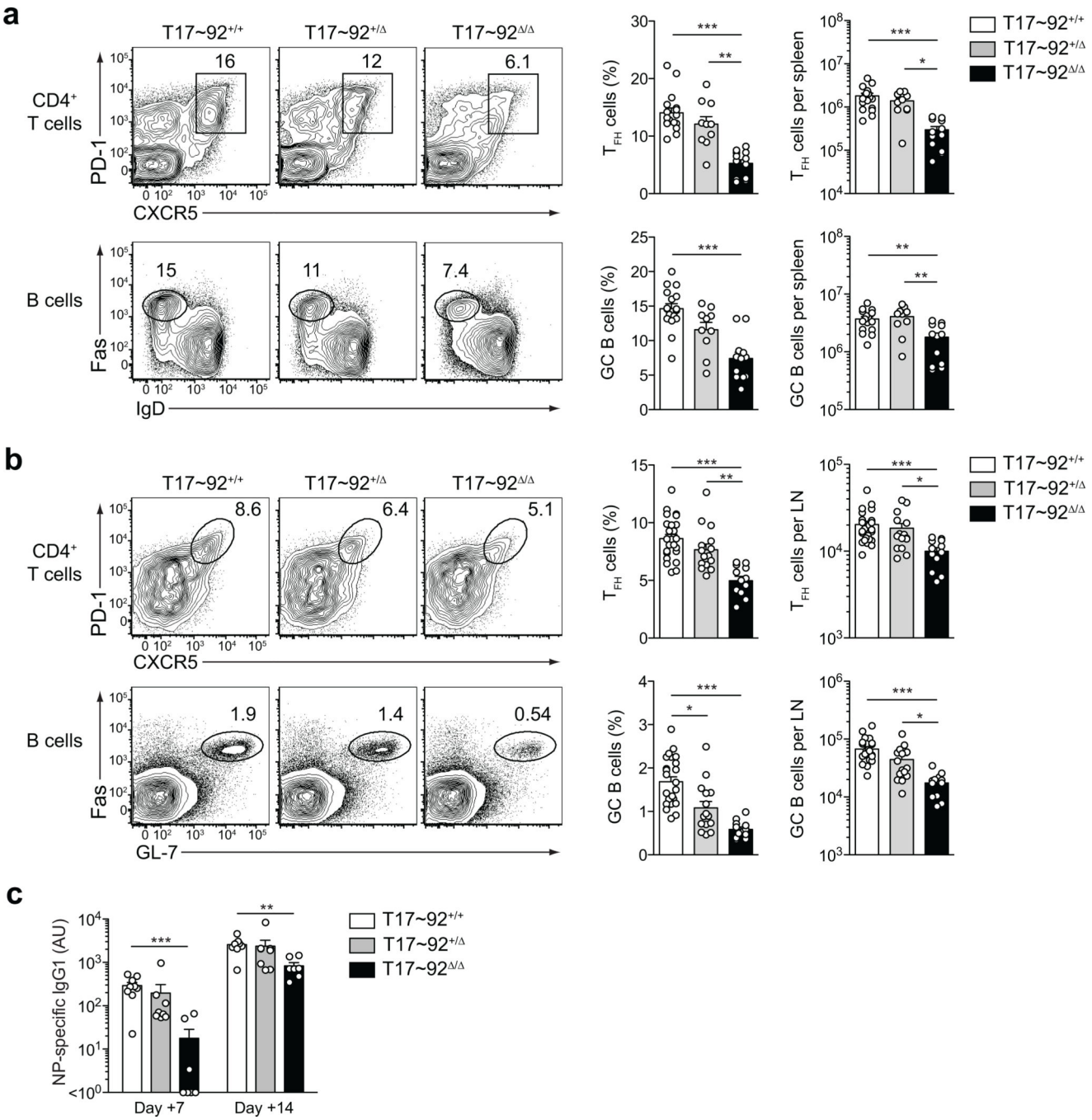

Figure 2. miR-17~92 regulates T_{FH} and germinal center responses

(**a**) CD4-Cre^{+}miR-17~92$^{+/+}$ or CD4-Cre^{-}miR-17~92$^{fl/fl}$ control mice (referred to as T17~92$^{+/+}$), CD4-Cre^{+}miR-17~92$^{+/fl}$ (T17~92$^{+/\Delta}$), and CD4-Cre^{+}miR-17~92$^{fl/fl}$ (T17~92$^{\Delta/\Delta}$) mice were infected intraperitoneally (i.p.) with LCMV Armstrong. Spleens were dissected on day +8 after infection and analyzed by flow cytometry. Representative contour plots show the frequency of CXCR5^{hi}PD-1^{hi} T_{FH} cells among CD4^{+} T cells (top panels) as well as the frequency of FAS^{+}IgD^{low} GC B cells among CD19^{+}B220^{+} B cells (bottom panels). Frequencies and total T_{FH} and GC B cell numbers are quantified in the bar

graphs. Data are pooled from three independent experiments and each dot represents one mouse (n = 12–17). (**b**) T17~92$^{+/+}$ control, T17~92$^{+/\Delta}$, and T17~92$^{\Delta/\Delta}$ mice were immunized s.c. with NP-OVA/alum in the hind foot pads. Draining LNs were analyzed by flow cytometry on day +7. Contour plots show the percentage of T_{FH} cells among activated (CD44^{hi}) CD4^{+} T cells (top panels) as well as the percentage of FAS^{+}GL-7^{+} GC B cells among CD19^{+}B220^{+} B cells. Frequencies and total T_{FH} and GC B cell numbers are quantified in the bar graphs. Data are pooled from three independent experiments and each dot represents one mouse (n = 12–24). (**c**) NP-specific serum IgG1 antibody levels (arbitrary units, AU) of NP-OVA/alum immunized T17~92$^{+/+}$ control, T17~92$^{+/\Delta}$, and T17~92$^{\Delta/\Delta}$ mice. Data are representative of two independent experiments.

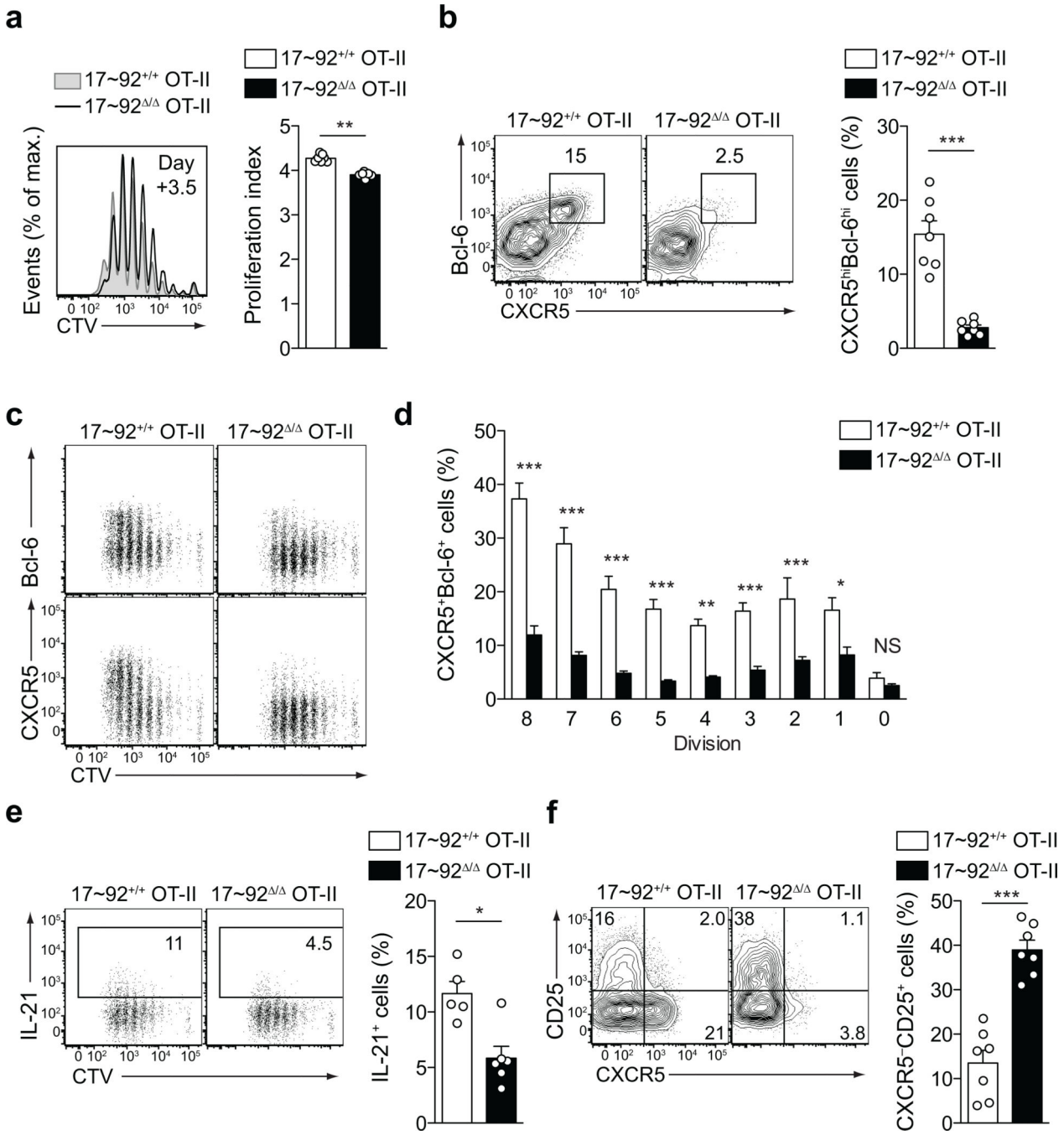

Figure 3. miR-17~92 is required for robust T_{FH} cell differentiation

(**a**) Naïve OT-II cells derived from T17~92$^{+/+}$ control and T17~92$^{\Delta/\Delta}$ mice were labeled with CTV and adoptively transferred into wild-type recipients, followed by NP-OVA/alum immunization in the hind footpads. Draining popliteal LNs were dissected on day +3.5 after immunization and analyzed by flow cytometry. Representative histogram overlays show CTV dilution of transferred control (grey shaded) and miR-17~92$^{\Delta/\Delta}$ (black line) OT-II cells. The proliferation index for each replicate is quantified in the bar graph (n = 7). (**b**) Representative contour plots and quantification of CXCR5^{hi}Bcl-6^{hi} T_{FH} cells among the

transferred OT-II cells. (**c**) Representative dot plots show Bcl-6 and CXCR5 expression kinetics of dividing OT-II cells on day +3.5. (**d**) Frequency of Bcl-6 and CXCR5 double-positive OT-II cells in relation to their cell division status (n = 7 mice). (**e**) Representative dot plots and quantification of IL-21-producing OT-II cells. (**f**) Representative contour plots and quantification of $CXCR5^{-}CD25^{+}$ OT-II cells. Data are representative of five (**a-d, f**) and two (**e**) independent experiments.

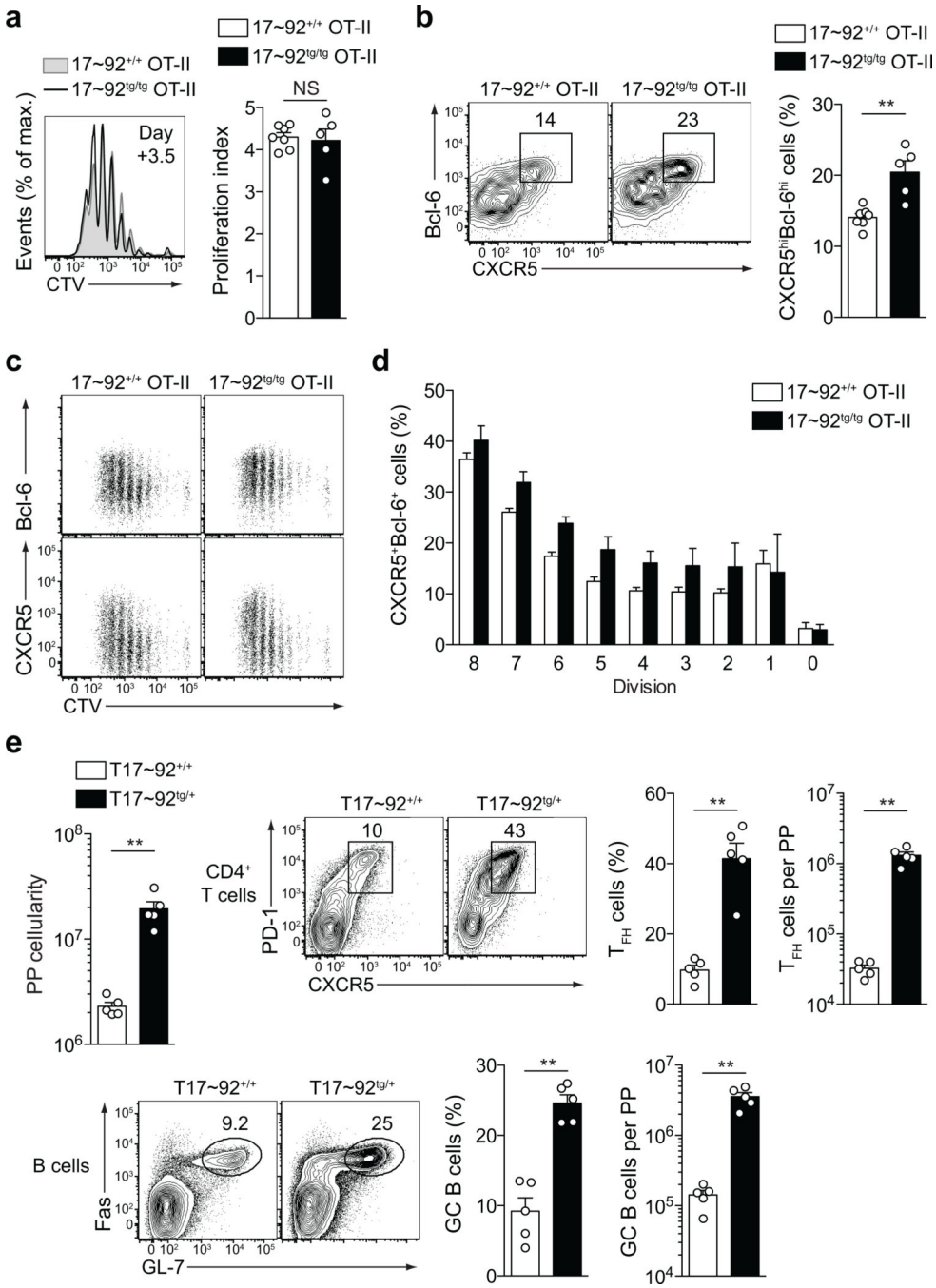

Figure 4. T cell-intrinsic miR-17~92 cluster overexpression promotes T_{FH} cell differentiation

(**a**) Naïve OT-II cells derived from T17~92$^{+/+}$ control and CD4-Cre^{+}Rosa-26-miR-17~92$^{tg/tg}$ (miR-17~92$^{tg/tg}$) mice were labeled with CTV and adoptively transferred into wild-type recipients, followed by NP-OVA/alum immunization in the hind footpads. Representative histogram overlays show CTV dilution of transferred control (grey shaded) and miR-17~92$^{tg/tg}$ (black line) OT-II cells on day +3.5. The proliferation index for each replicate is quantified in the bar graph (n = 5–7). (**b**) Quantification of CXCR5^{hi}Bcl-6^{hi} T_{FH} cells among the transferred OT-II cells. (**c**) Bcl-6 and CXCR5 expression kinetics of

dividing OT-II cells on day +3.5. (**d**) Frequency of Bcl-6 and CXCR5 double-positive OT-II cells in relation to their cell division status (n = 5–7 mice). Data are representative of four independent experiments. (**e**) Peyer's patches (PPs) were isolated from 10-week-old, unimmunized control (T17~92$^{+/+}$) and CD4-Cre^{+}miR17~92$^{tg/+}$ (T17~92$^{tg/+}$) mice and analyzed by flow cytometry. To allow for comparison of total PP cellularity, equal numbers of PPs were collected for each mouse. Representative contour plots show the frequency of CXCR5^{hi}PD-1^{hi} T_{FH} cells among CD4^{+} T cells and the frequency of FAS^{+}GL-7^{+} GC B cells among CD19^{+} B cells. Data is quantified in the bar graphs (n = 5).

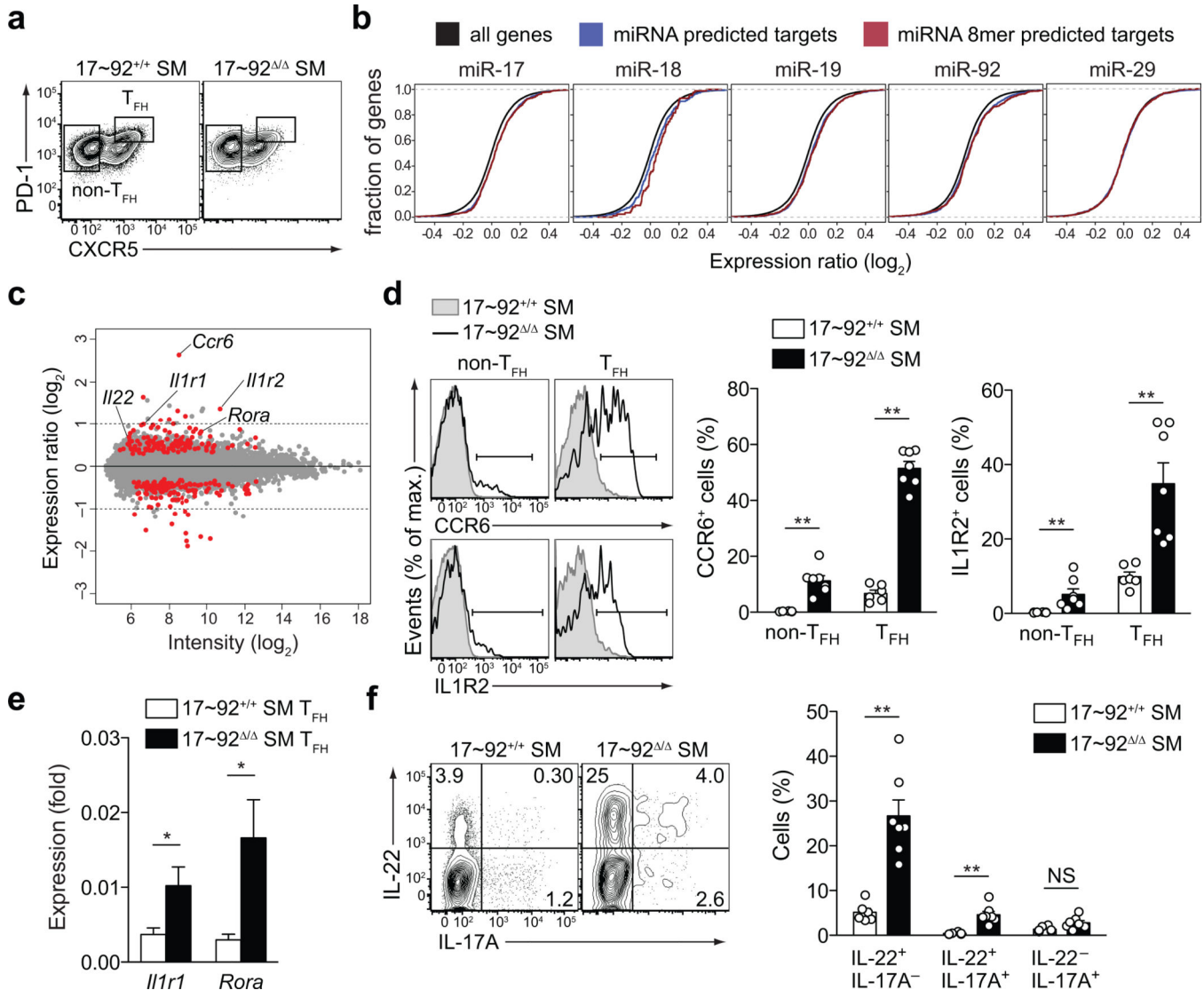

Figure 5. miR-17~92 enforces fidelity of the T_{FH} cell gene expression program

(**a**) Naïve LCMV-specific SMARTA (SM) cells derived from T17~92$^{+/+}$ control and T17~92$^{\Delta/\Delta}$ mice were adoptively transferred into wild-type recipients, followed by i.p. LCMV Armstrong infection. Spleens were dissected on day +5.5 after infection and analyzed by flow cytometry for identification of CXCR5^{hi}PD-1^{hi} T_{FH} and CXCR5^{-} non-T_{FH} cells. (**b**) Genome-wide transcriptome analysis of 17~92$^{\Delta/\Delta}$ and 17~92$^{+/+}$ control SMARTA T_{FH} cells on day +5.5 post LCMV Armstrong infection. The graphs display the $\log_2$ value of the gene expression ratio of 17~92$^{\Delta/\Delta}$ divided by 17~92$^{+/+}$ cells for each gene (x-axis) plotted against the cumulative fraction of all $\log_2$ ratios (y-axis). The curves show the values for all genes (black), computationally predicted miRNA target genes for the miRNA indicated above each plot (blue) or the genes with computationally predicted 8mer seed matches (red). Computationally predicted miR-29 target genes are shown as a negative control. (**c**) MA plot shows genome-wide transcriptome analysis of 17~92$^{\Delta/\Delta}$ and 17~92$^{+/+}$ control SMARTA T_{FH} cells with significantly upregulated and downregulated genes (raw $p<0.01$) marked in red. Selected T_{FH} subset-inappropriate genes upregulated in the 17~92$^{\Delta/\Delta}$

SMARTA T_{FH} cells are depicted. (**d**) Histograms show CCR6 and IL1R2 expression by non-T_{FH} and T_{FH} (as defined by the gates shown in (a)) 17~92$^{+/+}$ control and 17~92$^{\Delta/\Delta}$ SMARTA cells on day +5.5 after LCMV infection. Data are quantified in the bar graphs with each dot representing one mouse (n = 6–7). (**e**) Analysis of *Il1r1* and *Rora* expression in 17~92$^{+/+}$ control and 17~92$^{\Delta/\Delta}$ SMARTA T_{FH} cells on day +5.5 after LCMV infection. Expression was normalized to *Hprt1* (n = 5). (**f**) Quantification of the relative numbers of IL-22- and/or IL-17A–producing 17~92$^{+/+}$ control and 17~92$^{\Delta/\Delta}$ SMARTA cells on day +5.5 post infection following restimulation with PMA/ionomycin (n = 6–7).

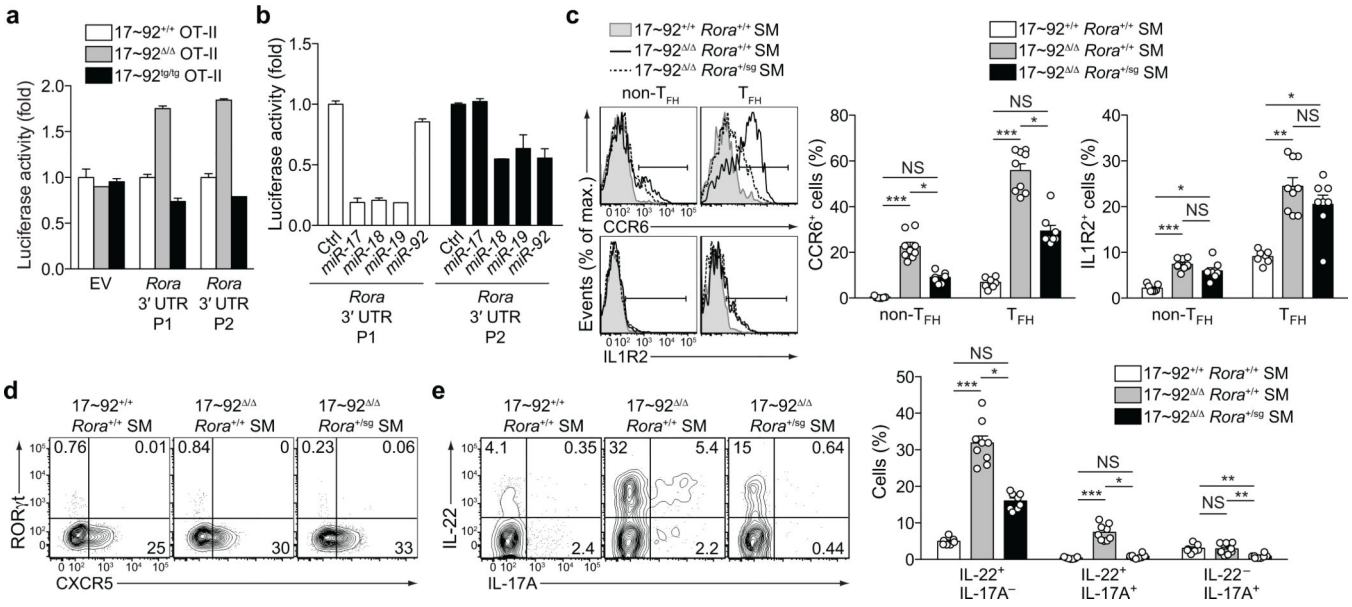

Figure 6. RAR-related orphan receptor alpha (*Rora*) is a functionally relevant miR-17~92 target

(**a**) *In vitro* stimulated OT-II cells from T17~92$^{+/+}$ control, T17~92$^{\Delta/\Delta}$, and T17~92$^{tg/tg}$ mice were transfected with dual luciferase reporters that contained mouse 3' UTR P1 or P2 of *Rora* (compare **Methods** and Supplementary Fig. 7 for details). Transfection with empty vector (EV) served as control. Renilla luciferase activity was measured 24 hours after transfection and normalized to firefly luciferase activity in transfected 17~92$^{+/+}$ control OT-II cells. Data are representative of three independent experiments. (**b**) Primary CD4-Cre^{+}Dgcr8$^{fl/fl}$ CD4^{+} T cells were used for co-transfection with 3' UTR P1 or P2 dual luciferase reporters and with the indicated miR-17~92 cluster miRNA or control miRNA mimics. Renilla luciferase activity was measured 24 hours after transfection and normalized to firefly luciferase activity. Values are relative to normalized luciferase in control-transfected cells. Data are representative of two independent experiments. (**c**) Naïve LCMV-specific SMARTA (SM) cells derived from T17~92$^{+/+}$*Rora*$^{+/+}$ control, T17~92$^{\Delta/\Delta}$*Rora*$^{+/+}$ or T17~92$^{\Delta/\Delta}$*Rora*$^{+/-}$ mice were adoptively transferred into wild-type recipients, followed by i.p. LCMV infection. Histograms show CCR6 and IL1R2 expression by non-T$_{FH}$ and T$_{FH}$ SMARTA cells of the indicated genotypes on day +5.5 after LCMV infection. Data are quantified in the bar graphs with each dot representing one mouse (n = 7–9). (**d**) Representative contour plots show RORγt and CXCR5 expression among SMARTA cells of the indicated genotypes. (**e**) Quantification of IL-22- and/or IL-17A–producing SMARTA cells on day +5.5 post infection following restimulation with PMA/ionomycin (n = 7–9).